Protein Science (1996), 5:1907–1916. Cambridge University Press. Printed in the USA.

Coupling between *trans/cis* proline isomerization and protein stability in staphylococcal nuclease

DAGMAR M. TRUCKSES,[1] JOHN R. SOMOZA,[2,3] KENNETH E. PREHODA,[1] STEPHEN C. MILLER,[1,4] AND JOHN L. MARKLEY[1]

[1]Department of Biochemistry, College of Agricultural and Life Sciences, University of Wisconsin–Madison, Madison, Wisconsin 53706
[2]Graduate Group in Biophysics, University of California at Berkeley, Berkeley, California 94720

(RECEIVED February 12, 1996; ACCEPTED June 27, 1996)

Abstract

The nucleases A produced by two strains of *Staphylococcus aureus*, which have different stabilities, differ only in the identity of the single amino acid at residue 124. The nuclease from the Foggi strain of *S. aureus* (by convention nuclease WT), which contains His^{124}, is 1.9 kcal·mol^{-1} less stable (at pH 5.5 and 20 °C) than the nuclease from the V8 strain (by convention nuclease H124L), which contains Leu^{124}. In addition, the population of the *trans* conformer at the Lys^{116}–Pro^{117} peptide bond, as observed by NMR spectroscopy, is different for the two variants: about 15% for nuclease WT and 9% for nuclease H124L. In order to improve our understanding of the origin of these differences, we compared the properties of WT and H124L with those of the H124A and H124I variants. We discovered a correlation between effects of different residues at this position on protein stability and on stabilization of the *cis* configuration of the Lys^{116}–Pro^{117} peptide bond. In terms of free energy, approximately 17% of the increase in protein stability manifests itself as stabilization of the *cis* configuration at Lys^{116}–Pro^{117}. This result implies that the differences in stability arise mainly from structural differences between the *cis* configurational isomers at Pro^{117} of the different variants at residue 124. We solved the X-ray structure of the *cis* form of the most stable variant, H124L, and compared it with the published high-resolution X-ray structure of the *cis* form of the least stable variant, WT (Hynes TR, Fox RO, 1991, *Proteins Struct Funct Genet 10*:92–105). The two structures are identical within experimental error, except for the side chain at residue 124, which is exposed in the models of both variants. Thus, the increased stability and changes in the *trans/cis* equilibrium of the Lys^{116}–Pro^{117} peptide bond observed in H124L relative to WT are due to subtle structural changes that are not observed by current structure determination techniques. Residue 124 is located in a helix. However, the stability changes are too large and follow the wrong order of stability to be explained simply by differences in helical propensity. A second site of conformational heterogeneity in native nuclease is found at the His^{46}–Pro^{47} peptide bond, which is approximately 80% *trans* in both WT and H124L. Because proline to glycine substitutions at either residue 47 or 117 remove the structural heterogeneity at that position and increase protein stability, we determined the X-ray structures of H124L+P117G and H124L+P47G+P117G and the kinetic parameters of H124L, H124L+P47G, H124L+P117G, and H124L+P47G+P117G. The individual P117G and P47G mutations cause decreases in nuclease activity, with k_{cat} affected more than K_m, and their effects are additive. The P117G mutation in nuclease H124L leads to the same local conformational rearrangement described for the P117G mutant of WT (Hynes TR, Hodel A, Fox RO, 1994, *Biochemistry 33*:5021–5030). In both P117G mutants, the loop formed by residues 112–117 is located closer to the adjacent loop formed by residues 77–85, and residues 115–118 adopt a type I′ β-turn conformation with the Lys^{116}–Gly^{117} peptide bond in the *trans* configuration, as compared with the parent protein in which these residues have a typeVI_a β-turn conformation with the Lys^{116}–Pro^{117} peptide bond in the *cis* configuration. Addition of the P47G mutation appears not to cause any additional structural changes. However, the electron density for part of the loop containing this peptide bond was not strong enough to be interpreted.

Keywords: enzyme activity; global protein stability; guanidinium chloride denaturation; helix stability; NMR spectroscopy; proline isomerization; staphylococcal nuclease; X-ray crystallography

Reprint requests to: John L. Markley, Department of Biochemistry, College of Agricultural and Life Sciences, University of Wisconsin—Madison, 420 Henry Mall, Madison, Wisconsin 53706; e-mail: markley@nmrfam.wisc.edu.
[3] Present address: Department of Biochemistry and Biophysics, University of California, San Francisco, California 94143-0448.
[4] Present address: Department of Pharmaceutical Chemistry, University of California, San Francisco, California 94143-0446.

Structural fluctuations in proteins occur on different time scales. Among the slowest are those that arise from Xxx–Pro peptide bond *trans/cis* isomerizations, with typical time constants in the range of ten to several hundred seconds. The role of Xxx–Pro peptide bond isomerizations in the kinetics of protein folding has been investigated thoroughly, and it is now widely accepted that such isomerizations are often the reason for slow steps in protein folding reactions (Kim & Baldwin, 1982, 1990). Similarly, there is substantial evidence that this isomerization can play an important role in protein function (Brown et al., 1977; Marsh et al., 1979; Dunker, 1982; Brandl & Deber, 1986; Touchette et al., 1986; Langsetmo et al., 1989). Therefore, determining the detailed structural and thermodynamic consequences of proline *trans/cis* isomerizations, as well as protein structural properties that influence *trans/cis* equilibria at Xxx–Pro peptide bonds, is of great interest to investigators. Proline residues are often found in loops and turns of proteins. The limited backbone flexibility of proline probably restrains the conformation and flexibility of a loop. Thus far, with systems exhibiting Xxx–Pro heterogeneities, protein structure determination methods have not provided full structures of both conformers: one with a *trans*-proline and the other with a *cis*-proline peptide bond. However, in several cases, it has been possible to characterize structural differences by NMR spectroscopy (Fox et al., 1986; Evans et al., 1987, 1989; Higgins et al., 1988; Chazin et al., 1989; Loh et al., 1991). Such phenomena have been studied most extensively in staphylococcal nuclease, where measurable populations of both the *cis* and *trans* configurations have been detected at the Lys^{116}–Pro^{117} and His^{46}–Pro^{47} peptide bonds (Evans et al., 1987; Loh et al., 1991). The relative intensities of doubled resonances assigned to the $^1H^{\epsilon 1}$ protons of histidines 8, 121, and 124 and the doubled resonances assigned to the $^1H^{\epsilon 1}$ protons of histidine 46 provide an easy measure of the *trans/cis* equilibria of the Lys^{116}–Pro^{117} and the His^{46}–Pro^{47} peptide bonds, respectively. In nuclease WT, approximately 90% of the molecules have a *cis* Lys^{116}–Pro^{117} peptide bond and approximately 20% have a *cis* His^{46}–Pro^{47} peptide bond.

Recently, the conformation of the loop formed by residues 112–117 in nuclease, containing Pro^{117}, has been analyzed in detail. A model peptide for this region, designed to approximate the unfolded state, showed the *trans/cis* equilibrium to be 24 (Raleigh et al., 1992). Thus, noncovalent intramolecular forces serve to perturb the Lys^{116}–Pro^{117} peptide bond equilibrium from predominantly *trans* in the unfolded protein to predominantly *cis* in the folded wild-type protein. Analysis of the structure suggested that these noncovalent interactions consist of hydrogen bonds on the C-terminal side and hydrogen bonding and packing interactions on the N-terminal side of the 112–117 loop (Hinck, 1993; Hodel et al., 1993, 1994). They anchor this loop to the body of the protein and act to stabilize the *cis* configuration of the Lys^{116}–Pro^{117} peptide bond (Hodel et al., 1993, 1994): the anchoring is thought to impose greater strain on the backbone of the loop in molecules with a *trans* Lys^{116}–Pro^{117} peptide bond than in those with the *cis* configuration (Hodel et al., 1993).

Nuclease has been isolated from both the Foggi and V8 strains of *Staphylococcus aureus* (Cusumano et al., 1968; Cone et al., 1970). These two nucleases differ at residue 124 in the third helix of the nuclease structure. Whereas the Foggi strain nuclease (WT) contains a histidine, the V8 strain nuclease (H124L) contains a leucine at this position. Depending on solution conditions, H124L is between 1.2 and 1.9 kcal·mol^{-1} more stable than WT (Shortle, 1986; Tanaka et al., 1993). Also, the population with a *trans* Lys^{116}–Pro^{117} peptide bond is approximately a factor of two smaller in H124L than in WT (Alexandrescu et al., 1990; Hinck, 1993). In order to investigate the structural origins of these differences, we solved the X-ray structure of H124L and compared it with the refined X-ray structure of WT (Hynes & Fox, 1991). The results showed that the structures are identical, at the limit of resolution, except at residue 124, the side chain of which is exposed in both. These observations suggest that the H124L mutation causes subtle changes in tertiary interactions that influence the conformation of loop residues 112–117 and result in a more stable protein. In order to improve our understanding of these changes, we also examined the protein stabilities and *trans/cis* ratios of the Lys^{116}–Pro^{117} peptide bond in the H124I and H124A nuclease variants. They are intermediate between the values for histidine and leucine.

In order to further analyze factors determining the conformation of the β-turns containing Pro^{47} and Pro^{117}, we solved the X-ray structures of H124L+P117G and H124L+P47G+P117G. The Pro to Gly mutations force the peptide bond into the *trans* configuration, thus eliminating the *trans/cis* peptide bond heterogeneity.

In a separate study (Hinck et al., 1996), we introduced pairs of cysteines into nuclease as a means of altering folded-state strain, according to whether the engineered disulfide is oxidized or reduced. This system also exhibited coupling between protein stability and the fractional *cis* configuration at the Lys^{116}–Pro^{117} peptide bond.

Results

Peptide bond trans/cis ratios

As mentioned in the Introduction, the $^1H^{\epsilon 1}$ resonances of His^8, His^{121}, and His^{124} in the NMR spectrum of nuclease report on the Lys^{116}–Pro^{117} peptide bond *trans/cis* equilibrium (Evans et al., 1987; Alexandrescu et al., 1988), and the $^1H^{\epsilon 1}$ resonances of His^{46} report on the His^{46}–Pro^{47} peptide bond *trans/cis* equilibrium (Loh et al., 1991). Figure 1 compares the histidine $^1H^{\epsilon 1}$ region of the ^1H NMR spectra of WT, H124L, and H124L+P117G. Comparison of the ratio of the areas of the peaks assigned to the *trans* and *cis* forms shows a greater *trans* population in WT compared with H124L. As expected, H124L+P117G exhibits only one peptide bond configuration at Lys^{116}–Pro^{117}, but maintains heterogeneity at the His^{46}–Pro^{47} peptide bond. The equilibrium constants for the Lys^{116}–Pro^{117} peptide bond *trans/cis* equilibrium of WT, H124A, H124I, and H124L are shown in Table 1. The free energy difference between the folded protein with the *trans* and with the *cis* Lys^{116}–Pro^{117} peptide bond was calculated from the NMR data (Fig. 2) for each of the variants at residue 124.

Protein stabilities

The stabilities of WT, H124A, H124I, H124L, H124L+P117G, H124L+P47G, and H124L+P47G+P117G were determined by guanidinium chloride (GdmCl) denaturation. The results are summarized in Table 1. The stability of the H124 variants increases in the order WT < H124A < H124I < H124L. The free energy difference between unfolded and folded protein, ΔG°_u, correlates with the relative free energy difference between molecules with the *trans* and *cis* configuration of the Lys^{116}–Pro^{117} peptide bond, $\Delta G^\circ_{trans/cis}$ (Fig. 2).

At 20 °C and pH 5.5, the P117G and P47G mutations increase the protein stability by 1.5 and 0.9 kcal·mol^{-1}, respectively. On

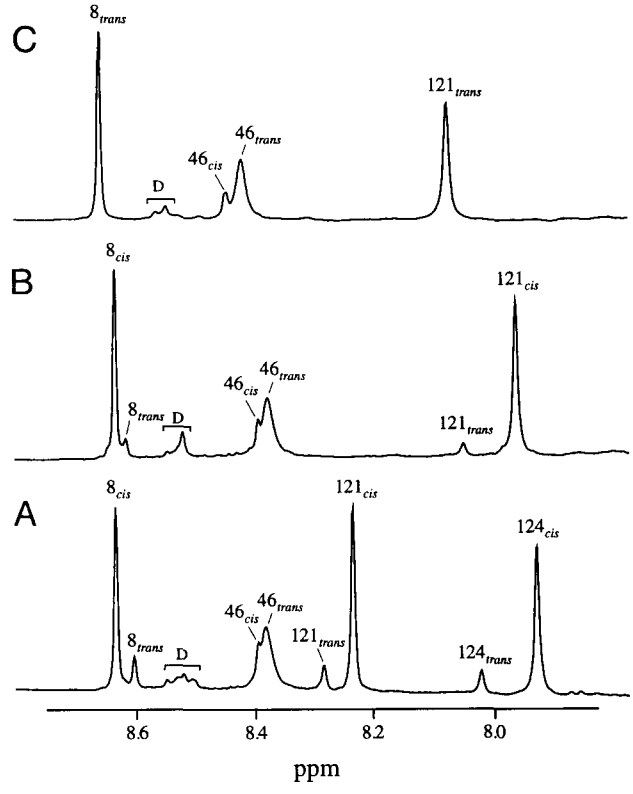

Fig. 1. Histidine $^1H^{\epsilon 1}$ proton region of the NMR spectra of staphylococcal nuclease variants. Splittings of the His^8, His^{121}, and His^{124} resonances due to *trans/cis* isomerization of the Lys^{116}–Pro^{117} peptide bond and splitting of His^{46} resonances due to isomerization of the His^{46}–Pro^{47} peptide bond are indicated. D denotes histidine $^1H^{\epsilon 1}$ peaks from denatured protein. **A:** WT. **B:** H124L. **C:** H124L+P117G.

first consideration, a proline-to-glycine mutation would be expected to decrease the stability of a protein because of a greater increase in the entropy of the denatured state compared with the native state (Némethy et al., 1966). However, changes in the native state caused by the mutation often lead to an overall stabilizing effect (Matthews et al., 1987; Yutani et al., 1991; Herning et al., 1992), as is the case for the P117G and P47G mutations in nuclease. Assuming that a proline-to-glycine substitution stabilizes the denatured state by 1.9 kcal·mol^{-1} (Némethy et al., 1966; Herning et al., 1992), the observed 1.5 kcal·mol^{-1} and 0.9 kcal·mol^{-1} net stabilizations, respectively, for P117G and P47G imply that these mutations lower the energy of the native state by 3.4 kcal·mol^{-1} and 2.8 kcal·mol^{-1}, respectively. However, the stability increases due to the P47G and P117G mutations are not additive. The stability of the double mutant is intermediate between those of the single mutants.

Sedimentation equilibrium

As a control for possible aggregation of the nuclease variants studied, sedimentation equilibrium data were collected. For each of three different centrifugation speeds, the plot of the natural log of the absorbance versus the squared radius yielded straight lines for the three measured variants (WT, H124A, and H124I), suggesting that only one molecular species was present in solution. The fit of the data yielded a molecular weight close to that of the nuclease monomer. From the plot of absorbance versus radius from the center of rotation, it was estimated that the highest protein concentration in the cell was approximately 0.4 mM. No multimeric species appeared to be present at this concentration.

Enzyme activity

The enzyme activities of H124L, H124L+P47G, H124L+P117G, and H124L+P47G+P117G were analyzed at pH 9.5 (the pH optimum of WT nuclease activity) in the presence of Ca^{2+}, using thymidine 3′-phosphate 5′-(*p*-nitrophenyl phosphate) as a substrate. The observed values of k_{cat}, K_m, and k_{cat}/K_m are summarized in Table 2. The P117G and P47G mutations each cause a small (sevenfold) decrease in nuclease activity; each mutation has a small effect on k_{cat} as well as on K_m. These changes appear to be additive, leading to a decrease in activity of the double proline mutant (P47G + P117G) by a factor of about 50.

Crystal structures

We determined high-resolution X-ray structural models for nuclease H124L, H124L+P117G, and H124L+P47G+P117G. Final refinement statistics and a description of the crystals are shown in Table 3.

Superposition of the X-ray structure of H124L with that of WT (1STN; Hynes & Fox, 1991) resulted in an RMS deviation (RMSD) of 0.16 Å between C^α carbons. These structures are essentially identical. The backbone conformation around residue 124 is not affected by the mutation, and the side chain of this residue is solvent exposed and has the same orientation in both variants (Kinemage 1), i.e., the χ^1 angles of this residue in the two structures are nearly identical. As in the structure of WT, the loop residues 42–53 have higher *B*-factors than the rest of the protein, suggesting greater flexibility for this part of the protein. Nevertheless, following refinement of the structure of H124L, this loop exhibited the same conformation in H124L as in WT.

Nuclease H124L+P117G shares the same overall fold with WT and H124L. However, the structures of H124L+P117G and H124L differ in conformation near the mutation site. The positions of residues 112–117 with respect to the rest of the protein are different in the two variants; in H124L+P117G, these residues are closer to the loop formed by adjacent residues 77–85 (Kinemage 2). Residues 115–118, which form a type VI_a β-turn in H124L and WT, adopt a type I′ β-turn in H124L+P117G, with the Lys^{116}–Gly^{117} peptide bond in the *trans* configuration. The side chains of Tyr^{115} and Lys^{116} are oriented differently in the two variants: in H124L, they point away from the rest of the protein and into solution; in H124L+P117G (Kinemage 2), they point into the active site, as described by Hynes et al. (1994) for P117G. Although residues 112–114 are located differently in the structures of H124L+P117G and P117G, they adopt the same extended conformation as in H124L and WT. Similarly, although the conformation of the loop formed by residues 77–85 is the same in all four structures, it is closer to the loop formed by residues 112–117 in H124L+P117G and P117G than in WT and H124L. This shift is maximal for Gly^{79}, whose backbone position has moved by 0.9 Å (Kinemage 2). A water molecule appears to be involved in stabilizing this new local arrangement. It forms a bridge by hydrogen bonding to the Tyr^{115} side chain hydroxyl group on one loop and

Table 1. *Thermodynamic parameters for guanidinium chloride denaturation of nuclease variants of staphylococcal nuclease and experimental values for the trans/cis ratios of the Lys^{116}–Pro^{117} peptide bond*[a]

Nuclease variant	C_m (M)[b]	m (kcal·mol^{-1}·M^{-1})[c]	ΔG°_u (kcal·mol^{-1})[d]	*Trans/cis* at residues 116–117
WT	0.77 ± 0.05	5.6 ± 0.3	4.3 ± 0.2	0.173 ± 0.002[e]
H124A	0.94 ± 0.06	5.3 ± 0.3	5.0 ± 0.2	0.136 ± 0.004[e]
H124I	0.98 ± 0.01	5.91 ± 0.05	5.8 ± 0.1	0.124 ± 0.004[e]
H124L	1.08 ± 0.03	5.8 ± 0.1	6.2 ± 0.1	0.097 ± 0.009[e]
P117G[f]	0.97	6.08	5.9 ± 0.2	[g]
H124L+P117G	1.29 ± 0.03	5.9 ± 0.1	7.7 ± 0.1	[g]
H124L+P47G	1.21 ± 0.02	5.88 ± 0.03	7.1 ± 0.1	[g]
H124L+P47G+P117G	1.41 ± 0.01	5.28 ± 0.05	7.4 ± 0.1	[g]

[a] Experimental conditions were 200 mM sodium acetate, pH 5.5, 20 °C. The results represent averages of three experiments for each variant. Indicated errors for ΔG°_u and m represent one standard deviation from the mean.
[b] C_m represents the [GdmCl] at which half of the protein is denatured.
[c] m is the slope of the graph of ΔG°_u versus [GdmCl].
[d] ΔG°_u is the extrapolated stability at 0 M GdmCl.
[e] *Trans/cis* ratios of the Lys^{116}–Pro^{117} peptide bond were obtained from the ratio of the areas under the histidine $^1H^{\epsilon 1}$ proton resonances of His^{121}.
[f] The C_m and ΔG°_u values for P117G are from Hynes et al. (1994). The m-value for this variant was calculated from those values.
[g] The Lys^{116}–Pro^{117} peptide bond is fully *trans*.

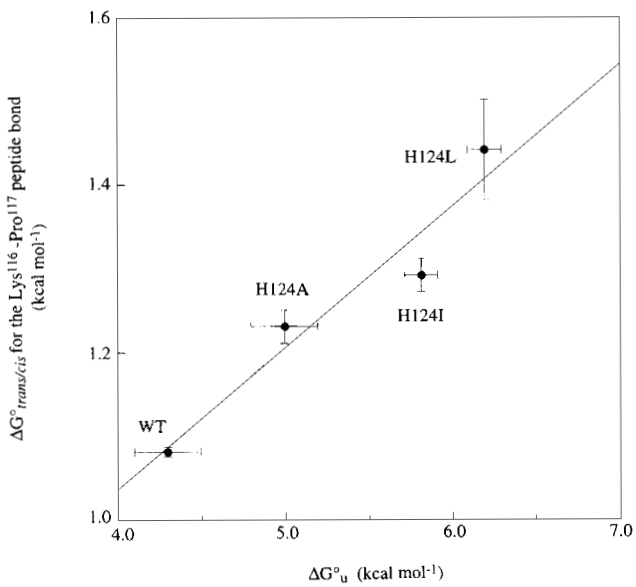

Fig. 2. Plot showing the correlation between the free energy for the configurational equilibrium between the *trans* and *cis* forms of the Lys^{116}–Pro^{117} peptide bond ($\Delta G^\circ_{trans/cis}$) and for the equilibrium between the folded and unfolded form of the protein (ΔG°_u) in variants of staphylococcal nuclease with different residues at position 124 as indicated in the figure. ΔG°_u was determined from GdmCl denaturation as monitored by fluorescence (see Materials and methods). Errors represent one standard deviation from the average of three or four measurements. $\Delta G^\circ_{trans/cis}$ was calculated from the relative populations of the *trans* and *cis* states as determined from the integrals of the doubled $^1H^{\epsilon 1}$ NMR resonances of His^{121} for the respective mutant (Evans et al., 1987; Alexandrescu et al., 1988). Indicated error represents one standard deviation from the average of three measurements.

to the side chain of Gln^{80} and the backbone carbonyl oxygen of Thr^{82} on the other loop (Kinemage 2; Fig. 3); the water oxygen is in the same plane as the tyrosine ring, and the angle between the tyrosine C–O bond and the water oxygen is 120 degrees, as is expected for this kind of hydrogen bond (Ippolito et al., 1990).

Table 2. *Kinetic parameters for the hydrolysis of thymidine 3′-phosphate 5′-(p-nitrophenyl phosphate) catalyzed by H124L and mutant staphylococcal nucleases*[a]

Nuclease variant	K_m (mM)	k_{cat} (min^{-1})	k_{cat}/K_m (mM^{-1} min^{-1})
H124L	0.074 ± 0.003	17 ± 3	226 ± 37
H124L+P47G	0.104 ± 0.007	3.4 ± 0.1	33 ± 2.5
H124L+P117G	0.120 ± 0.007	3.9 ± 0.1	32 ± 20
H124L+P47G+P117G	0.30 ± 0.02	1.3 ± 0.1	4.4 ± 0.4

[a] Assay conditions were 0.1 M CHES, 0.2 M KCl, 0.1 M $CaCl_2$, pH 9.5, 26 °C. Indicated errors represent the estimated uncertainties in the fit of the data to Michaelis–Menten kinetics.

In the structure of H124L+P117G, the electron density is weak for the flexible loop formed by residues 42–53 and is discontinuous for residues 45–50. Because no electron density was seen for these six residues throughout the refinement, they were not included in the model. The other residues in this loop refined to a somewhat different conformation in H124L+P117G than in H124L and WT, suggesting a different local conformation. However, because this part of the protein is not well defined by the data, these differences cannot be interpreted unambiguously.

Except for loop residues 42–53, which are not well defined, the X-ray structures of H124L+P47G+P117G and H124L+P117G are essentially identical. The RMSD between backbone atoms of the two structures, excluding residues 42–53, is 0.14 Å. Similarly, the H124L+P117G and H124L+P47G+P117G structures differ from the WT P117G structure (1SYC; Hynes et al., 1994) only in the flexible loop (residues 42–53). For the reasons described above, we did not attempt to interpret these differences further.

Solvent-excluded volumes

Recently, there has been renewed interest in studying the partial molar volume changes, $\Delta V^\circ_{unfolding}$, accompanying protein folding

Table 3. *Final refinement statistics and parameters*

	H124L	H124L+P117G	H124L+P47G+P117G
Protein residues included in the refinement	6–141	6–44, 51–141	6–44, 51–141
Number of non-hydrogen protein atoms	1,090	1,039	1,039
Number of water molecules	69	32	25
Crystallographic parameters:			
Space group	$P4_1$	$P4_1$	$P4_1$
Cell parameters (Å):			
a, b	47.74	49.01	49.18
c	63.71	63.66	63.51
Resolution range (Å)	6.0–1.7	6.0–1.95	6.0–1.95
Total number of measurements	91,144	36,225	30,773
Number of unique reflections ($\|F\| > 0.0\sigma$)	15,599	11,126	10,604
Number of unique reflections ($\|F\| > 2.0\sigma$)	13,478	10,171	9,523
% Completeness of unique reflections (Å)	98.8 (∞–1.7)	98.9 (∞–1.95)	94.5 (∞–1.95)
% Completeness in highest resolution shell (Å)	97.6 (1.75–1.7)	97.1 (2–1.95)	90.0 (2–1.95)
R_{merge} (%)[a]	5.90	6.20	4.74
R-factor for $\|F\| > 2.0\sigma$ (%)	17.0	18.4	18.7
Free R-factor for $\|F\| > 2.0\sigma$ (%)	22.4	25.5	27.4
Mean B-factor (Å^2):			
Protein backbone atoms	23.8	34.6	49.9
Protein side-chain atoms	28.3	38.2	53.5
Water atoms	38.2	41.5	51.7
RMSDs from ideal geometry:			
Bond lengths (Å)	0.009	0.010	0.011
Bond angles (degrees)	1.693	1.632	1.602
Dihedral angles (degrees)	22.866	22.730	24.112
Improper angles (degrees)	1.225	1.218	1.380

[a] $R_{merge}(I) = \{\Sigma_{hkl}|I(h,k,l) - \langle I(h,k,l)\rangle|/\ \Sigma_{hkl}\ I(h,k,l)\} \times 100\%$.

(Weber & Drickamer, 1983; Silva & Weber, 1993; Gross & Jaenicke, 1994; Prehoda & Markley, 1996). The size of $\Delta V^{\circ}_{\text{unfolding}}$ is determined by differences in the solvent-excluded volume and by volume differences due to differences in protein-solvent interactions between the native and the denatured states. The P117G mutation in nuclease is at the surface of the protein and does not disrupt hydrophobic interactions. Thus, it seems reasonable that any changes in $\Delta V^{\circ}_{\text{unfolding}}$ are due to changes in the solvent-excluded volume. Initial results (Royer et al., 1993) suggested that proline to glycine mutations make the protein more compact, i.e., that they cause a decrease in the solvent-excluded volume of the native state of nuclease. However, more recent experimental data (Vidugiris et al., 1996) indicated that the $\Delta V^{\circ}_{\text{unfolding}}$ values for H124L and H124L+P117G are identical within experimental error. We calculated the solvent-excluded volumes of H124L and H124L+P117G in the native (X-ray structures) and unfolded (modeled by extended chain) states using the PQMS program by Connolly (1985) (Table 4). The calculated native-state volume of

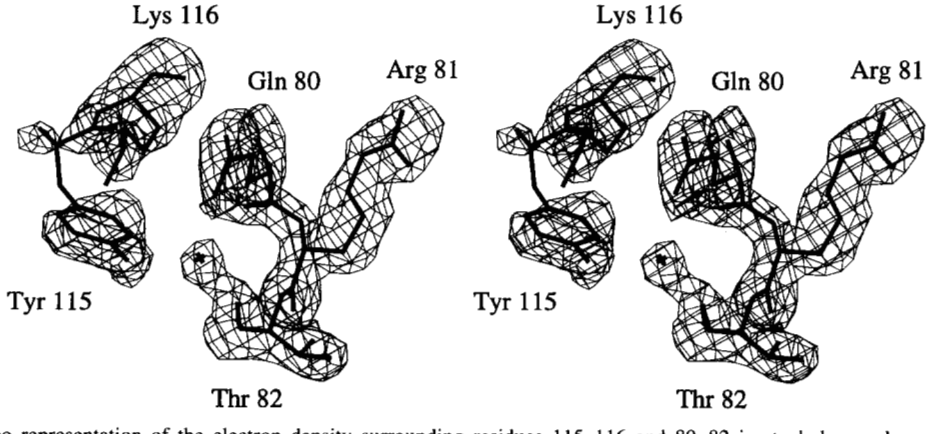

Fig. 3. Stereo representation of the electron density surrounding residues 115–116 and 80–82 in staphylococcal nuclease mutant H124L+P117G. The figure shows an SA-omit $F_o - F_c$ map (Hodel et al., 1992) calculated using the final refined model with residues 115–116, 80–82, and the water molecule omitted. The map was contoured at 1.8σ.

Table 4. *Solvent-excluded volumes of H124L and H124L+P117G*

Nuclease variant	Solvent-excluded volume ($mL \cdot mol^{-1}$)
H124L (native)	9,909
H124L (denatured)	7,622
H124L+P117G (native)	9,861
H124L+P117G (denatured)	7,603

H124L+P117G is approximately 48 $mL \cdot mol^{-1}$ smaller than that of H124L. Similarly, the denatured-state volume of H124L+P117G is approximately 20 $mL \cdot mol^{-1}$ smaller than that of H124L, as expected from the three additional carbon atoms present in a proline compared with a glycine. Assuming that the effects of solvation are equivalent for the two variants and because the error in these calculations is estimated to be approximately 20 $mL \cdot mol^{-1}$, these calculations are consistent with the more recent experimental results that the P117G mutation does not cause significant changes in $\Delta V^{\circ}_{unfolding}$.

Discussion

Xxx–Pro peptide bonds in polypeptides are unique because the energy of the *cis* configuration of these bonds is closer to that of the *trans* than in other peptide bond linkages. In random coil polypeptides, the population of *cis* Xxx–Pro bonds varies between 5% and 30% (Brandts et al., 1975; Grathwohl & Wüthrich, 1976; Juy et al., 1983; Raleigh et al., 1992). The size of this population is influenced mainly by the identity of neighboring residues. In highly structured proteins, however, the protein fold can have a significant impact on the population, often leading to a predominant *cis* configuration in type VI reverse turns. In this article, we attempt to further analyze factors involved in stabilizing particular conformations in proline-containing loops of nuclease and to determine their relationship to the global protein stability.

From extensive studies of the Lys^{116}–Pro^{117} peptide bond in nuclease (Alexandrescu et al., 1989, 1990; Hinck, 1993; Hodel et al., 1993, 1994, 1995), a generalization has emerged concerning the dependence of the configuration of the 116–117 peptide bond on solution conditions or residue substitutions at positions external to the 112–117 loop: if the change destabilizes the protein, it destabilizes the *cis* configuration of the Lys^{116}–Pro^{117} peptide bond; conversely, if it stabilizes the protein, it stabilizes the *cis* configuration. Mutations at Lys^{116} do not follow these rules; in fact, the relationship between the stability of the *cis* configuration and the global protein stability appears to be reversed. For example, K116G has a *trans* Gly^{116}–Pro^{117} peptide bond, yet it is more stable than WT (Hodel et al., 1993). An explanation for this is that mutations that introduce flexibility at residue 116 reduce the strain otherwise present when the Pro^{117} peptide bond is *trans*.

It is easy to rationalize how mutations at sites near Pro^{117} affect the configuration of its peptide bond. However, it is more difficult to explain the influence of mutations farther away in the protein structure, particularly at residues whose side chains are not involved in tertiary interactions. Their effect on the *trans/cis* ratio of the Lys^{116}–Pro^{117} peptide bond must be a manifestation of the cooperativity in the protein fold.

His^{124} is located on the solvent-exposed side of the helix adjacent to the loop containing the Lys^{116}–Pro^{117} peptide bond and is not involved in tertiary interactions. Mutation of this residue to Ala, Ile, and Leu stabilizes the *cis* configuration of the Lys^{116}–Pro^{117} peptide bond, following the expected correlation with protein stability (Fig. 2), the more stabilizing mutation favoring the *cis* configuration more. The slope of the correlation indicates that the energy required for the perturbation of the *trans/cis* ratio at the Lys^{116}–Pro^{117} peptide bond represents approximately 17% of the overall observed stabilization energy of each of the substitutions at residue 124. In order to investigate these effects, it is important to determine whether they may arise from protein aggregation. Because protein stability appears to increase as a function of the hydrophobicity of residue 124, the increase in stability might be due to differential dimerization of the protein. Our sedimentation equilibrium results, however, show no evidence for dimerization. Moreover, the decrease in protein stability at higher protein concentrations, observed by calorimetry (Tanaka et al., 1993), has been explained by dimerization in the denatured state rather than in the native state. Thus, dimerization effects of residue 124 mutations probably are destabilizing rather than stabilizing. The calorimetric results indicate that the unfolded-state dimer is more stable for nuclease H124L than for WT, suggesting that the more hydrophobic residue 124 mutations favor denatured state dimerization.

Although the *cis* and *trans* configurational states in the folded protein are at equilibrium with those of the unfolded protein, a perturbation of the *trans/cis* ratio in the folded state can only be explained by relative changes in chemical potentials within the folded state. A relative increase in the population of the *cis* state can be explained by stabilization of the folded structure with a *cis* Lys^{116}–Pro^{117} peptide bond, a destabilization of the folded structure with a *trans* peptide bond, or both. Because destabilization of the *trans* state in the folded protein would lead to overall destabilization of the protein, which is not observed, the major effect must be on the chemical potential of the *cis* state. Because this is the state observed in the X-ray structures, it was hoped that comparison of the structures of WT and H124L would reveal a mechanism for stabilization. For example, some hydrogen bond that is important in stabilizing the *cis* configuration might be present in H124L but not in WT. However, the crystal and solution (Wang J, Truckses DM, Dzukula Z, Zolnai Z, Markley JL, in prep.) structures of nuclease H124L do not show any such obvious structural difference from the X-ray structure of WT (Hynes & Fox, 1991). Because no differences in the structural models were observed, the shift in the *trans/cis* ratio of the Lys^{116}–Pro^{117} peptide bond must be caused by subtle structural changes that can not be detected by current structure determination techniques.

The model of Hodel et al. (1993) attributes the higher population of the *cis* species at the 116–117 peptide bond to strain induced in the loop containing Pro^{117} when the peptide bond is *trans*, by its anchorage to the rest of the protein. If, as is suggested here, the energy of the *trans* configuration is unaffected by mutations that alter the *trans/cis* ratio, then the strain (higher energy) induced in the loop must be offset equally by favorable interactions (lower energy) in the rest of the protein. Thus, the important factor in determining the position of the *trans/cis* ratio is the differential energy of the variant when the peptide bond is *cis*. Variants with a lower *trans/cis* ratio are ones characterized by more favorable interactions in the *cis* configuration that lower its energy (Alexandrescu et al., 1988).

Considering the molecular origin of the thermodynamic stability increase due to the mutations might provide further insight into the

structural differences that lead to the changes in the *trans/cis* equilibrium. Residue 124 is located in a helix. Previous investigations of the effects on protein stability of amino acid substitutions in helical regions have revealed several relevant factors: the helical propensity of the amino acid, the position within the helix (center or near the ends), and/or interactions of the amino acid with other residues within the helix and/or with the rest of the protein (Horovitz et al., 1992; Blaber et al., 1993, 1994; Pinker et al., 1993).

In our case, residue 124 is in the fourth position of helix 3 formed by residues 121–135; i.e., it is located at the N-terminal end of the helix. The histidine has a positive charge (at the pH of the measurements) that probably interacts unfavorably with the helix dipole at this position, leading to destabilization of the helix. This unfavorable interaction is eliminated with leucine at this position. Support for this idea comes from the observation that the H124L mutation stabilizes the protein more at pH 5.0 than at pH 7.0 (1.9 kcal·mol^{-1} compared to 1.3 kcal·mol^{-1}) (Tanaka et al., 1993). Another consideration is a possible interaction between His^{124} and another charged side chain. The nearest charge-bearing residue is His^{121}. However, the side chains of these two histidines are more than 6 Å apart, and each is surrounded by solvent. Also the pK_a of His^{121} is not higher in H124L than in WT (Alexandrescu et al., 1988), as would be expected if there was a charge–charge interaction between these two histidines. Thus, an unfavorable interaction between these two residues seems unlikely.

A final consideration is the relative helical propensity of the amino acid at residue 124. Model studies suggest the following values for global protein stabilization due to mutation of an intrahelical histidine (Blaber et al., 1993): His → Ile, 0.27 kcal·mol^{-1}; His → Leu, 0.35 kcal mol^{-1}; and His → Ala, 0.39 kcal·mol^{-1}. Helical propensities determined from host–guest model studies agree with this order of stabilization (O'Neil & DeGrado, 1990; Lyu et al., 1990), but the values are somewhat different: His → Ile, 0.17 kcal·mol^{-1}; His → Leu, 0.54 kcal·mol^{-1}; and His → Ala, 0.71 kcal·mol^{-1}. Our studies show that these replacements at residue 124 in nuclease result in larger stabilizations than predicted from the model studies, especially for His → Ile and His → Leu. Also, the order of stability is different than expected from helical propensity values. Therefore, simple helical propensity of the mutated residue does not adequately explain the observed changes in global protein stability.

Unfolding of nuclease WT has been shown to be a three-state process under conditions of low pH (pH 4.1) and high salt concentration (>100 mM NaCl) (Carra et al., 1994; Carra & Privalov, 1995). Our stability measurements were performed in 200 mM sodium acetate, at pH 5.5. It seems unlikely that our GdmCl titration studies are monitoring only partial unfolding rather than the full denaturation transition because the stability values determined here are in agreement with those obtained under different solution conditions and monitored by different probes (Shortle, 1986; Royer et al., 1993; Tanaka et al., 1993).

The P117G mutation causes a major change in the conformation and orientation of the loop formed by residues 112–117. The configuration of the Lys^{116}–Gly^{117} peptide bond is *trans*, as expected because of the greater energetic cost of introducing a *cis* peptide bond configuration in a non-prolyl peptide bond. The conformation adopted by this loop is independent of the H124L substitution, as shown by comparison of the structures of H124L+P117G (present work) and P117G (Hynes et al., 1994). Also, the P117G mutation stabilizes the protein to the same extent in nuclease WT and H124L. The greater conformational flexibility of glycine compared with proline probably results in decoupling of the loop conformation from the domain containing residue 124, thus abolishing the cooperativity between these two parts of the protein.

Materials and methods

Protein sample preparation

Mutants of nuclease H124L were created by introducing site-directed base changes in the cloned gene (Hinck, 1993). All nuclease variants were then produced in *Escherichia coli* using the T7 expression system. The host BL21(DE3) contained the appropriate T7 expression vector and the plasmid pLysS. Nuclease was isolated and purified by procedures described previously (Royer et al., 1993). The protein samples were estimated to be greater than 95% pure according to SDS-polyacrylamide gels.

Protein stability

The stability of the nuclease variants was measured by following the intrinsic fluorescence of the single tryptophan at residue 140 as a function of GdmCl concentration at 20 °C and pH 5.5. Each sample contained approximately 75 μg/mL protein in 200 mM sodium acetate, pH 5.5, with varying amounts of GdmCl. The tryptophan was excited at 295 nm, and fluorescence emission was monitored at 340 nm with an ISS Koala spectrofluorometer (ISS, Urbana, Illinois). The apparent unfolding equilibrium constants as a function of GdmCl were extracted from the data (Shortle & Meeker, 1986), and an estimate of ΔG_u° for protein unfolding in the absence of denaturant was obtained by extrapolation to zero denaturant concentration (Pace, 1975). Unfolding of each variant was conducted three times. Average values are reported, and indicated errors represent one standard deviation from the average.

Sedimentation equilibrium

Sedimentation equilibrium experiments with nuclease WT, H124A, and H124I were performed using a Beckman Optima XL-A analytical ultracentrifuge. Experimental conditions were the same as for the stability measurements, except that protein concentrations were 0.2 mg/mL and no GdmCl was used. Equilibrium distributions at rotation speeds of 25,000, 33,000, and 37,000 rpm were examined by detecting absorbance at 280 nm. The natural log of the absorbance was plotted versus the radius square and fitted to $(\partial \ln A)/\partial r^2 = [M(1 - \rho v)\omega^2]/2RT$, where M is the molecular weight, ρ is the density of the solution, v is the partial specific volume, A is the absorbance, and r is the radius from the center of rotation.

Crystallography

Crystals of all nuclease variants were obtained using a modification of the conditions and method described by Loll and Lattman (1989). Lyophilized protein was dissolved in filtered 10.5 mM potassium phosphate buffer, pH 8.15; the protein concentration was 20 mg/mL. Freshly distilled, filtered 2-methyl-2,4-pentanediol (MPD) (Eastman Kodak Company) was added slowly with mixing to the protein solution, to a final concentration of 17% (w/w). This solution was allowed to sit at 4 °C for at least 24 h and then was centrifuged to eliminate precipitated protein. Vapor diffusion trays were set up with the wells containing solutions ranging between 20–30% MPD (w/w) in 10.5 mM potassium phosphate, pH 8.15. Crystals of the space group $P4_1$ grew within one to two weeks (Table 3). X-ray diffraction intensities were recorded on a Rigaku

R-AXIS II C area detector and reduced using the R-AXIS data processing software. A single crystal was used for each of the three described data sets. Further details of the data collection and reduction are described in Table 3.

Refinement of the nuclease variant structures was performed with X-PLOR versions 3.0 and 3.1 (Brünger, 1992). A round of refinement typically consisted of positional refinement, simulated annealing, repeated positional refinement, individual atomic *B*-factor refinement, and manual fitting of the model into electron density maps. Whereas the models of the H124L and the H124L+P117G variants were fitted using $2F_o - F_c$ and $F_o - F_c$ maps generated by X-PLOR, most maps of the H124L+P47G+P117G variant were generated by the holographic method (Somoza et al., 1995). X-PLOR maps were used only for the final rounds of refinement of this mutant. Model changes were carried out with the PS FRODO software package (Jones, 1985) on an Evans & Sutherland PS390 graphics display. Following initial rigid-body refinement, each structure was refined with approximately 9% of the data omitted for calculation of the free *R*-factor (Brünger, 1993). Only reflections greater than $2\sigma(F_o)$ were included in the refinement. Water molecules were added into positive, spherical $F_o - F_c$ density in each model and were kept in the model if their *B*-factors remained below 60 Å^2 and if they were within reasonable hydrogen bonding distance of a hydrogen bond donor or acceptor. Because the crystals of all three variants diffracted more strongly along the c^* axis than along the a^* and b^* axes, the structure factors F_o in each case were scaled with an optimized overall anisotropic *B*-factor. Details of the refinement of each structure are described below, and the RMSDs from ideal geometry as well as the *R*-factors of the final models are reported in Table 3.

The structure of the H124L+P47G+P117G mutant was solved by molecular replacement and refined using the uncomplexed WT nuclease crystal structure (Hynes & Fox, 1991) as a starting model (Somoza et al., 1995). During initial refinement, residues surrounding the mutations (residues 45–50, 116–118, and 123–125) were omitted. As refinement progressed, residues 116–118 and 123–125 were fitted into the electron density. Residues 115–118 initially were refined in a type II′ β-turn conformation. However, $F_o - F_c$ density and no $2F_o - F_c$ density was visible for the carbonyl oxygen of Lys^{116}. Readjustment of residues 115–118 into a type I′ β-turn conformation resulted in a better fit. Residues 45–50 were not included in the model because only little discontinuous electron density was visible for these residues throughout the refinement.

The structure of H124L+P47G+P117G without residues 45–50 and without water molecules was used as a starting model for the refinement of the H124L+P117G structure. The initial *R*-factor, which was 25.2% (data between 6.0 and 1.95 Å), dropped to 22.4% after the first round of refinement; at this stage the free *R*-factor was 26.8% (data between 6.0 and 1.95 Å). As in the case of the H124L+P47G+P117G model, little discontinuous $F_o - F_c$ density for residues 45–50 was visible throughout the refinement; therefore, these residues were not included in the model.

The structure of H124L was refined using as a starting model the uncomplexed WT nuclease model (Hynes & Fox, 1991) without water molecules. The *R*-factor after rigid-body refinement was 52.4%. A 180 degree rotation, yielded by a rotation search, resulted in an *R*-factor of 25.4% (data between 6.0 and 2.0 Å resolution) after further adjustment of the orientation with rigid body refinement. Residues 45–50 and 123–125 were excluded during the first round of refinement, which lowered the *R*-factor to 23.4% and resulted in a free *R*-factor of 27.9% (data between 6.0 and 1.7 Å resolution). Water molecules were incorporated during the following rounds of refinement, and a leucine was fitted into $F_o - F_c$ density at residue 124, after which residues 123–125 were included in the refinement. Fairly clear $F_o - F_c$ density was also present for residues 45–50. Thus, these residues were included in the model.

The coordinates of the structures of H124L, H124L+P117G, and H124L+P47G+P117G have been submitted for deposit at the Protein Data Bank (Brookhaven); ID codes 1SND, 1SNP, and 1SNQ.

Molecular volume calculation

The molecular solvent-excluded volumes of the H124L and the H124L+P117G X-ray structures were calculated using the PQMS program (Connolly, 1985, 1993). In this calculation, the molecule is modeled as a static collection of hard spheres that completely exclude a spherical probe representing the solvent. A probe radius of 1.4 Å was used. The solvent-excluded volumes of the same proteins in the unfolded state were calculated similarly. For this purpose, the protein chain was unfolded by setting all ϕ and ψ angles to 180 degrees. Errors in these calculations are estimated to be 20 mL·mol^{-1}.

NMR spectroscopy

Protein dissolved in 99.9% D_2O was heated to 50 °C for approximately 40 min to exchange amide protons with deuterium. Then sodium acetate-d_3 dissolved in D_2O, pH 5.5, was added to a final buffer concentration of 200 mM. The sample was lyophilized, redissolved in 100% D_2O, and the pH was adjusted to 5.3 (uncorrected for deuterium isotope effects). The sample was centrifuged to eliminate any precipitant and transferred to an NMR tube. All samples contained approximately 1 mM EDTA to chelate any leftover metal ions in solution. Protein concentrations were between 2 and 2.5 mM. One-dimensional ^{1}H NMR spectra were recorded on a 500 MHz Bruker spectrometer with a DMX console. The spectral width was approximately 6,009 Hz, with a data size of 8,192 total points. The number of averaged transients was 4,096 or 8,192 (eight initial "dummy scans" were discarded). NMR spectra were processed with the Felix computer program (BIOSYM/Molecular Simulations, Inc., San Diego, California). No apodization was applied, and the frequency spectra were baseline corrected with a second-order polynomial using a five-point interval. The line-fitting routine in Felix was used to obtain accurate integrals of the histidine $^1H^{\epsilon 1}$ resonances. They were fitted to a Lorentzian lineshape using a simulated annealing optimization method. Each spectrum was recorded three times, and each of these spectra was fitted three times in order to obtain an estimate of the uncertainty in the measurement.

Enzyme activity

The nuclease activities of the proline mutants were measured using the enzyme assay described by Grissom and Markley (1989). The initial rate of cleavage of *p*-nitrophenyl phosphate (PNP) from thymidine 3′-phosphate 5′-(PNP) was monitored at 330 nm with a Hewlett Packard 8452A diode array spectrophotometer. The extinction coefficient of PNP was assumed to be 9.4×10^3 M^{-1}cm^{-1} (Grissom & Markley, 1989). Assay conditions were 100 mM CHES, 200 mM KCl, and 100 mM $CaCl_2$ at pH 9.5 and 28 °C. The same substrate stock solution was used for all assays, and the experi-

ments were performed on the same day in order to minimize differences due to substrate degradation.

Acknowledgments

We thank Dr. Sung-Hou Kim, Chemistry Department at the University of California at Berkeley, for the use of an Evans & Sutherland graphics display system, as well as for access to the Rigaku R-AXIS II C area detector and computers; Dr. Catherine Royer, University of Wisconsin—Madison School of Pharmacy, for access to equipment for carrying out the fluorimetry experiments; Dr. Ivan Rayment, Institute of Enzyme Research at the University of Wisconsin—Madison, for use of his coldroom and equipment for growing and examining protein crystals; and Dr. Darrell McCaslin for help with sedimentation equilibrium experiments. This research was supported by grant GM 35976 from the National Institutes of Health (NIH). NMR studies were conducted at the National Magnetic Resonance Facility at Madison, whose operation is subsidized by grant RR02301 from NIH National Center for Research Resources and whose instrumentation was purchased with funds from the National Science Foundation (NSF), the University of Wisconsin—Madison, the NIH, and the U.S. Department of Agriculture. Sedimentation equilibrium experiments were done at the Biophysics Instrumentation Facility supported by NSF grant BIR 9512577. D.M.T. was supported in part by a fellowship administered by the Department of Biochemistry at the University of Wisconsin—Madison. S.C.M. was supported by a Hilldale Undergraduate/Faculty Research Award from the University of Wisconsin—Madison.

References

Alexandrescu AT, Hinck AP, Markley JL. 1990. Coupling between local structure and global stability of a protein: Mutants of staphylococcal nuclease. *Biochemistry 29*:4516–4525.

Alexandrescu AT, Mills DA, Ulrich EL, Chinami M, Markley JL. 1988. NMR assignments of the four histidines of staphylococcal nuclease in native and denatured states. *Biochemistry 27*:2158–2165.

Alexandrescu AT, Ulrich EL, Markley JL. 1989. Hydrogen-1 NMR evidence for three interconverting forms of staphylococcal nuclease: Effects of mutations and solution conditions on their distribution. *Biochemistry 28*:204–211.

Blaber M, Zhang X, Lindstrom JD, Pepiot SD, Baase WA, Matthews BW. 1994. Determination of α-helix propensity within the context of a folded protein. Sites 44 and 131 in bacteriophage T4 lysozyme. *J Mol Biol 235*:600–624.

Blaber M, Zhang X, Matthews BW. 1993. Structural basis of amino acid α helix propensity. *Science 260*:1637–1640.

Brandl CJ, Deber CM. 1986. Hypothesis about the function of membrane-buried proline residues in transport proteins. *Proc Natl Acad Sci USA 83*:917–921.

Brandts JF, Halvorson HR, Brennan M. 1975. Consideration of the possibility that the slow step in protein denaturation reactions is due to *cis-trans* isomerism of proline residues. *Biochemistry 29*:4953–4963.

Brown RD, Brewer CF, Koenig SH. 1977. Conformation states of concanavalin A: Kinetics of transitions induced by interactions with Mn^{2+} and Ca^{2+} ions. *Biochemistry 16*:3883–3896.

Brünger AT. 1992. X-PLOR Version 3.1: A system for x-ray crystallography and NMR. Yale University: New Haven.

Brünger AT. 1993. Assessment of phase accuracy by cross validation: The free *R* value. Methods and applications. *Acta Crystallogr D 49*:24–36.

Carra JH, Anderson EA, Privalov PL. 1994. Three-state thermodynamic analysis of the denaturation of staphylococcal nuclease mutants. *Biochemistry 33*:10842–10850.

Carra JH, Privalov PL. 1995. Energetics of denaturation and *m* values of staphylococcal nuclease mutants. *Biochemistry 34*:2034–2041.

Chazin WJ, Kördel J, Drakenberg T, Thulin E, Brodin P, Grundström T, Forsén S. 1989. Proline isomerism leads to multiple folded conformations of calbindin D_{9k}: Direct evidence from two-dimensional ^1H NMR spectroscopy. *Natl Acad Sci USA 86*:2195–2198.

Cone JL, Cusumano CL, Taniuchi H, Anfinsen CB. 1970. Staphylococcal nuclease (Foggi strain) II. The amino acid sequence. *J Biol Chem 246*:3103–3110.

Connolly ML. 1985. Computation of molecular volume. *J Am Chem Soc 107*:1118–1124.

Connolly ML. 1993. The molecular surface package. *J Mol Graphics 11*:139–141.

Cusumano CL, Taniuchi H, Anfinsen CB. 1968. Staphylococcal nuclease (Foggi strain) I. Order of cyanogen bromide fragments and a "fourth" histidine residue. *J Biol Chem 243*:4769–4777.

Dunker AK. 1982. A proton motive force transducer and its role in proton pumps, proton engines, tobacco mosaic virus assembly and hemoglobin allosterism. *J Theor Biol 97*:95–127.

Evans PA, Dobson CM, Kautz RA, Hatfull G, Fox RO. 1987. Proline isomerism in staphylococcal nuclease characterized by NMR and site-directed mutagenesis. *Nature 329*:266–270.

Evans PA, Kautz RA, Fox RO, Dobson CM. 1989. A magnetization-transfer nuclear magnetic resonance study of the folding of staphylococcal nuclease. *Biochemistry 28*:362–370.

Fox RO, Evans PA, Dobson CM. 1986. Multiple conformations of a protein demonstrated by magnetization transfer NMR spectroscopy. *Nature 320*:192–194.

Grathwohl C, Wüthrich K. 1976. The X-Pro peptide bond as an NMR probe for conformational studies of flexible linear peptides. *Biopolymers 15*:2025–2041.

Grissom CB, Markley JL. 1989. Staphylococcal nuclease active-site amino acids: pH dependence of tyrosines and arginines by ^{13}C NMR and correlation with kinetic studies. *Biochemistry 28*:2116–2124.

Gross M, Jaenicke R. 1994. Proteins under pressure. The influence of high hydrostatic pressure on structure, function and assembly of proteins and protein complexes. *Eur J Biochem 221*:617–630.

Herning T, Yutani K, Inaka K, Kuroki R, Matsushima M, Kikuchi M. 1992. Role of proline residues in human lysozyme stability: A scanning calorimetric study combined with X-ray structure analysis of proline mutants. *Biochemistry 31*:7077–7085.

Higgins KA, Craik DJ, Hall JG, Andrews PR. 1988. *Cis-trans* isomerization of the proline residue in insulin studied by ^{13}C NMR spectroscopy. *Drug Des and Del 3*:159–170.

Hinck AP. 1993. NMR investigation of a model proline *cis:trans* isomerization reaction in staphylococcal nuclease [thesis]. Madison, Wisconsin: University of Wisconsin.

Hinck AP, Truckses DM, Markley JL. 1996. Engineered disulfide bonds in staphylococcal nuclease: Effects on stability and conformational forms of the folded protein. *Biochemistry*. Forthcoming.

Hodel A, Kautz RA, Adelman DM, Fox RO. 1994. The importance of anchorage in determining a strained protein loop conformation. *Protein Sci 3*:549–556.

Hodel A, Kautz RA, Fox RO. 1995. Stabilization of a strained protein loop conformation through protein engineering. *Protein Sci 4*:484–495.

Hodel A, Kautz RA, Jacobs MD, Fox RO. 1993. Stress and strain in staphylococcal nuclease. *Protein Sci 2*:838–850.

Hodel A, Kim SH, Brünger AT. 1992. Model bias in macromolecular crystal structures. *Acta Crystallogr A 48*:851–858.

Horovitz A, Matthews JM, Fersht AR. 1992. α-Helix stability in proteins II. Factors that influence stability at an internal position. *J Mol Biol 227*:560–568.

Hynes TR, Fox RO. 1991. The crystal structure of staphylococcal nuclease refined at 1.7 Å resolution. *Proteins Struct Funct and Genet 10*:92–105.

Hynes TR, Hodel A, Fox RO. 1994. Engineering alternative β-turn types in staphylococcal nuclease. *Biochemistry* 33:5021–5030.

Ippolito JA, Alexander RS, Christianson DW. 1990. Hydrogen bond stereochemistry in protein structure and function. *J Mol Biol 215*:457–471.

Jones TA. 1985. Interactive computer graphics: FRODO. *Methods Enzymol 115*:157–171.

Juy M, Lam-Thanh H, Lintner K, Fermandjian S. 1983. Conformation and mobility of tyrosine side chain in tetrapeptides. Specific effects of *cis-* and *trans*-proline in Tyr-Pro- and Pro-Tyr- segments. *Int J Peptide Protein Res 22*:437–449.

Kim PS, Baldwin RL. 1982. Specific intermediates in the folding reactions of small proteins and the mechanism of protein folding. *Annu Rev Biochem 51*:459–489.

Kim PS, Baldwin RL. 1990. Intermediates in the folding reactions of small proteins. *Annu Rev Biochem 59*:631–660.

Langsetmo K, Fuchs J, Woodward C. 1989. *Escherichia coli* thioredoxin folds into two compact forms of different stability to urea denaturation. *Biochemistry 28*:3211–3220.

Loh SN, McNemar CW, Markley JL. 1991. Detection and kinetic characterization of a novel proline isomerism in staphylococcal nuclease by NMR spectroscopy. *Techniques in protein chemistry II*. New York: Academic Press, Inc. pp 275–282.

Loll PJ, Lattman EE. 1989. The crystal structure of the ternary complex of staphylococcal nuclease, Ca^{2+}, and the inhibitor pdTp, refined at 1.65 Å. *Proteins Struct Funct Genet 5*:183–201.

Lyu PC, Liff MI, Marky MI, Kallenbach NR. 1990. Side chain contributions to the stability of alpha-helical structure in peptides. *Science 250*:669–673.

Marsh HC, Scott ME, Hiskey RG, Koehler KA. 1979. The nature of the slow metal ion-dependent conformational transition in bovine prothrombin. *Biochem J 183*:513–517.

Matthews NW, Nicholson H, Becktel WJ. 1987. Enhanced protein thermosta-

bility from site-directed mutations that decrease the entropy of unfolding. *Proc Natl Acad Sci USA 84*:6663–6667.

Némethy G, Leach SJ, Scheraga HA. 1966. The influence of amino acid side chains on the free energy of helix-coil transitions. *J Phys Chem 70*:998–1004.

O'Neil KT, DeGrado WF. 1990. A thermodynamic scale for the helix-forming tendencies of the commonly occurring amino acids. *Science 250*:646–651.

Pace CN. 1975. The stability of globular proteins. *CRC Crit Rev Biochem 3*:1–43.

Pinker RJ, Lin L, Rose GD, Kallenbach NR. 1993. Effects of alanine substitutions in α-helices of sperm whale myoglobin on protein stability. *Protein Sci 2*:1099–1105.

Prehoda KE, Markley JL. 1996. Use of partial molar volumes of model compounds in the interpretation of high pressure effects on proteins. In: Markley JL, Royer CA, Northrop D, eds. *High-pressure effects in molecular biophysics and enzymology*. Oxford, UK: Oxford University Press. pp 33–43.

Raleigh DP, Evans PA, Pitkeathly M, Dobson CM. 1992. A peptide model for proline isomerism in the unfolded state of staphylococcal nuclease. *J Mol Biol 228*:338–342.

Royer CA, Hinck AP, Loh SN, Prehoda KE, Peng X, Jonas J, Markley JL. 1993. Effects of amino acid substitutions on the pressure denaturation of staphylococcal nuclease as monitored by fluorescence and nuclear magnetic resonance spectroscopy. *Biochemistry 32*:5222–5232.

Shortle D. 1986. Guanidine hydrochloride denaturation studies of mutant forms of staphylococcal nuclease. *J Cell Biochem 30*:281–289.

Shortle D, Meeker AK. 1986. Mutant forms of staphylococcal nuclease with altered patterns of guanidine hydrochloride and urea denaturation. *Proteins Struct Funct Genet 1*:81–89.

Silva JL, Weber G. 1993. Pressure stability of proteins. *Annu Rev Phys Chem 44*:89–113.

Somoza JR, Szöke H, Goodman DM, Béran P, Truckses D, Kim SH, Szöke A. 1995. Holographic methods in X-ray crystallography IV. A fast algorithm and its application to macromolecular crystallography. *Acta Crystallogr A 51*:708–716.

Tanaka A, Flanagan J, Sturtevant JM. 1993. Thermal unfolding of staphylococcal nuclease and several mutant forms thereof studied by differential scanning calorimetry. *Protein Sci 2*:567–576.

Touchette NA, Perry KM, Matthews CR. 1986. Folding of dihydrofolate reductase from *Escherichia coli*. *Biochemistry 25*:5445–5452.

Vidugiris GAJ, Truckses DM, Markley JL, Royer CA. 1996. High-pressure denaturation of staphylococcal nuclease proline-to-glycine substitution mutants. *Biochemistry 35*:3857–3864.

Weber G, Drickamer HG. 1983. The effect of high pressure upon proteins and other biomolecules. *Q Rev Biophys 16*:89–112.

Yutani K, Hayashi S, Sugisaki Y, Ogasahara K. 1991. Role of conserved proline residues in stabilizing tryptophan synthase α subunit: Analysis by mutants with alanine or glycine. *Proteins Struct Funct Genet 9*:90–98.